The analytic structure of the stationary kinetic boundary layer for Brownian particles near an absorbing wall

1991 J. Phys. A: Math. Gen. 24 4677

(http://iopscience.iop.org/0305-4470/24/19/027)

J. Phys. A: Math. Gen. 24 (1991) 4677-4695. Printed in the UK

The analytic structure of the stationary kinetic boundary layer for Brownian particles near an absorbing wall

A J Kainz and U M Titulaer

Institut für Theoretische Physik, Johannes Kepler Universität Linz, A-4040 Linz, Austria

Received 3 April 1991, in final form 11 June 1991

Abstract. A method for solving kinetic boundary layer problems for the (1D) Klein-Kramers equation, the kinetic equation for Brownian particles, was proposed a few years ago by Marshall and Watson for the special case of particles moving under the influence of a constant or zero external force. In this paper we apply this method to a number of classical stationary boundary layer problems for completely or partially absorbing walls. These are the Milne problem, in which a current flows towards the wall from infinity, and the albedo problem, in which particles are injected into the system at the wall with a prescribed velocity distribution. The solutions are known to be non-analytic at the wall for zero normal velocity; we pay particular attention to the nature of this singularity for several special cases. The results are compared with results obtained by approximate methods. The latter typically provide quicker and more accurate results for the distribution away from the singularity, due to the slow convergence of the series encountered in the Marshall-Watson approach. The latter is clearly superior, however, for determining the nature of the singularity and for calculating distribution functions and density profiles in its vicinity.

1. Introduction and survey

A few year ago, Marshall and Watson [1-3] used Wiener-Hopf techniques to treat the kinetic boundary layer for the 1D Klein-Kramers equation [4, 5], the kinetic equation for non-interacting Brownian particles diffusing in a background medium, for the special case of a completely absorbing wall and a spatially constant external force. Until then the only exactly solved boundary layer problems concerned variants of the linear BGK equation [6, 7 and references therein], in which the collision operator is replaced by a projection operator (or a finite sum of projection operators, all but one of finite-dimensional range). The solution by Marshall and Watson is therefore of great interest, both in its own right and as a test case for approximate methods developed to treat kinetic boundary layer problems for more general collision operators [8, 9 and references therein]. Thus it appears worthwhile to explore the content of this solution in somewhat more detail than was done in [1-3].

In contrast to the BGK case, boundary layer problems in the Klein-Kramers case are not reduced to quadratures. Instead, most quantities of interest are expressed as infinite series that in general converge rather slowly. This slow convergence is related [10] to a non-analyticity in the velocity distribution at the wall at zero normal velocity. The nature of this singularity had been determined before [10, 11]†, but its analysis is made much easier by the techniques developed by Marshall and Watson [1-3]. Since

† Some of the results of [10] were obtained independently by Mayya [12].

0305-4470/91/194677+19$03.50

results about the behaviour of the distribution function away from the non-analytic point can usually be obtained more economically and more accurately by variants of the moment method [8, 13], we shall concentrate in this paper on results concerning the distribution function for various boundary layer problems in the neighbourhood of the singularity; a more complete discussion of the results obtainable by analysis of the Marshall-Watson solution is given elsewhere [14].

In section 2 we formulate the basic equations and define the fundamental boundary layer problems, the Milne and the albedo problem. In addition we discuss two systems of solutions of the equation, the boundary layer eigenfunctions first introduced by Pagani [15, 16], as well as the basic solutions for a transformed equation used by Marshall and Watson for an 'inner expansion' around the singularity; the latter are given here in somewhat more detail than in [1-3]. Finally, we state the basic half-range orthogonality theorem derived in [1]. In section 3 we present some results for the Milne problem, in which a current flows from infinity towards the totally absorbing wall. In particular we compare the results obtained for small velocities by means of the inner expansion with results from a numerical simulation [17] and from variants of the moment method [8, 13].

In section 4 we discuss the albedo problem, in which particles are injected into the system at the wall and are reabsorbed once they return to the wall. Explicit numerical results are shown for the case where the distribution of the velocity u of the injected particles has the form $u^a \exp[-bu^2/2]$. Again, particular attention is paid to the velocity distribution of the returning particles for low velocities. In section 5 we discuss a variant of the Milne problem in which a fixed percentage of the particles is reflected specularly. This is known [11] to cause a change in the type of singularity of the velocity distribution at the wall. We determine this singularity both by a direct application of the inner expansion and by an expansion in the number of reflections undergone by the particle; the latter method amounts to adding to a Milne problem a number of albedo problems with injected distributions of the type $u^{1/2}(\ln u)^m$. The results are again compared with approximate results obtained by a moment method. The final section contains some concluding remarks, mainly on the utility of various approaches to kinetic boundary layers for the Klein-Kramers equation.

2. Basic equations and methods of solution

The Klein-Kramers equation for the distribution function $P(u, x, t)$ of the velocity u and the position x of an assembly of non-interacting Brownian particles in an external potential $V(x) = 2m\alpha x$ reads

$$\frac{\partial P}{\partial t} = \left[-u\frac{\partial}{\partial x} + 2\alpha\frac{\partial}{\partial u} \right] P + \gamma \left[\frac{1}{m\beta}\frac{\partial^2}{\partial u^2} + \frac{\partial}{\partial u}u \right] P \tag{2.1}$$

where m is the mass of the particle, γ its coefficient of friction and $\beta = (kT)^{-1}$ with T the temperature of the ambient medium. By using only one space and velocity component we have restricted ourselves to cases where the boundary conditions and the initial values do not depend on the 'transverse' space components, and where the distribution of transverse velocities is Maxwellian with inverse temperature β at all times; the latter condition may be relaxed somewhat [8]. In the remainder of this paper we shall use units such that $\gamma = m\beta = 1$. The Laplace transform $\hat{P}(u, x, s)$ of P obeys

the equation

$$\left[\frac{\partial}{\partial x}-\mathscr{A}(s)\right]\hat{P}(u,x,s)=\frac{1}{u}P(u,x,0) \tag{2.2}$$

where the operator $\mathscr{A}(s)$ is given by

$$\mathscr{A}(s)=\frac{1}{u}\frac{\partial}{\partial u}\left(u+2\alpha+\frac{\partial}{\partial u}\right)-\frac{s}{u}. \tag{2.3}$$

The operator $\mathscr{A}(s)$ is 'Hermitian' with respect to the indefinite scalar product

$$\langle f,g\rangle=\int_{-\infty}^{+\infty}\mathrm{d}u\,u\exp[\tfrac{1}{2}u^2+2\alpha u]f^*(u)g(u). \tag{2.4}$$

The eigenvalues and eigenfunctions of $\mathscr{A}(s)$ are known [18]:

$$\begin{aligned}&\mathscr{A}(s)\phi_n^\sigma(u)=-\lambda_{\sigma n}\phi_n^\sigma(u) \qquad \sigma=\pm 1 \qquad n=0,1,\ldots\\ &\lambda_{\sigma n}=\alpha+\sigma q_n \qquad q_n=[n+s+\alpha^2]^{1/2}\\ &\phi_n^\sigma(u)\equiv \mathrm{e}^{-\alpha u-u^2/2}f_n^\sigma(u)=\frac{1}{\sqrt{n!}}\mathrm{e}^{-\alpha u-u^2/4}D_n(2q_n-\sigma u)\end{aligned} \tag{2.5}$$

where $D_n(z)$ denotes the parabolic cylinder function, related to the Hermite polynomial $H_n(y)$ by

$$D_n(z)=2^{-n/2}\,\mathrm{e}^{-z^2/4}H_n(z/\sqrt{2}). \tag{2.6}$$

When α and s do not both vanish, all $\lambda_{\sigma n}$ are distinct, and the ϕ_n^σ obey the orthonormality relation

$$\langle\phi_n^\sigma,\phi_m^\tau\rangle=\sigma\sqrt{8\pi}\,q_n\delta_{\sigma\tau}\delta_{nm}. \tag{2.7}$$

The homogeneous solutions of (2.2) corresponding to (2.5) are

$$\psi_n^\sigma(u,x)=\phi_n^\sigma(u)\exp[-(\alpha+\sigma\sqrt{n+s+\alpha^2})x]. \tag{2.8}$$

For $\alpha, s\ll 1$, the $\psi_n^\sigma(u,x)$ with $n\neq 0$ change on a length scale of unity (in dimensional units: on the scale of the velocity persistence length $l=(\gamma\sqrt{m\beta})^{-1}$). The solutions with $n=0$ change much more slowly; they are solutions of Chapman–Enskog type [6]. For $s=0$, the ψ_n^σ with $\sigma=\operatorname{sgn}\alpha$ becomes the equilibrium distribution; the other one is constant in space, and one sees from (2.7) that it is the only one of the ψ_n^σ to carry a particle current. For $s=0$, $\alpha\to 0$ the two ψ_n^σ coalesce into the (unnormalized) Maxwell distribution:

$$\lim_{\alpha\downarrow 0}\psi_0^\sigma(u,x)=\phi_0(u)=\exp[-u^2/2]. \tag{2.9}$$

The operator $\mathscr{A}(0)$ acquires a Jordan associated function

$$\phi_0'(u)=\lim_{\alpha\downarrow 0}\frac{1}{2\alpha}[\phi_0^+(u)-\phi_0^-(u)]=u\exp[-u^2/2] \tag{2.10}$$

obeying

$$\mathscr{A}(0)\phi_0'(u)=-\phi_0(u). \tag{2.11}$$

The associated homogeneous solution of (2.2), normalized to unit negative current, is

$$\psi_0^c(u,x) = \lim_{\alpha \downarrow 0} \frac{1}{2\alpha\sqrt{2\pi}} [\phi_0^-(u) - \phi_0^+(u)\, e^{-2\alpha x}]$$

$$= \frac{x-u}{\sqrt{2\pi}} \exp[-u^2/2]. \tag{2.12}$$

The orthonormality relation (2.7) allows one to write any function $g(u)$ (provided the norm obtained by replacing u in (2.4) by $|u|$ is finite) as a *unique* linear combination of the $\phi_n^\sigma(u)$ (supplemented by $\phi_0'(u)$ for the case $s=\alpha=0$). Replacing the $\phi_n^\sigma(u)$ by the corresponding $\psi_n^\sigma(u,x)$ yields the unique homogeneous solution of (2.2) that assumes given boundary values $g(u;s)$ at the boundary $x=0$. However, in actual problems, only the $g(u;s)$ for particles *leaving* the source (at the wall) are given, whereas only the $\psi_n^\sigma(u,x)$ with $\sigma = \operatorname{sgn} x$ are acceptable building blocks for physically meaningful solutions (at least in the absence of sources at infinity). To construct such a solution one would need a set of functions biorthogonal to the $\varphi_n^\sigma(u)$ on the half-range $\sigma u > 0$. The existence of such a biorthogonal set was proved by Beals and Protopopescu [19]; their explicit construction was carried out by Marshal and Watson [1]. For convenience, we shall treat only the case $\sigma > 0$, and formulate the theorem in terms of the functions $f_n^\sigma(u)$, introduced in (2.5), rather than the $\phi_n^\sigma(u)$, in order to remain closer in our notation to earlier work; the f_n^σ obey an orthonormality relation similar to (2.7), but with the weight function in (2.4) replaced by $u \exp[-u^2/2]$. Thus we look for a system of functions $F_n^+(u)$, such that

$$\{F_n^+, f_m^+\} = \sqrt{8\pi}\, q_n \delta_{nm} \tag{2.13}$$

with

$$\{f, g\} = \int_0^\infty du\, u \exp[-u^2/2] f^*(u) g(u). \tag{2.14}$$

Marshall and Watson derived the explicit expression

$$F_n^+ = f_n^+ - \sum_{m=0}^{\infty} \frac{1}{2qm}\, \sigma_{nm} f_m^-(u) \tag{2.15}$$

with

$$\sigma_{nm} = [(q_n + q_m) Q_n Q_m]^{-1} \tag{2.16}$$

$$Q_n = \lim_{N\to\infty} \frac{[n!(N-1)!]^{1/2}}{N+n-1}\, e^{2q_n\sqrt{N}} \prod_{j=0}^{N+n-1} (q_j + q_n)^{-1}. \tag{2.17}$$

Via the q_n, the quantity Q_n also depends on the parameter $\tau = s + \alpha^2$, as is seen from (2.5). We shall therefore occasionally write it as $Q_n(\tau)$. The functions $F_n^+(u)$ vanish for $u < 0$ [1].

From the results just mentioned it follows that there is a unique solution of the homogeneous version of (2.2) of the form (for $x > 0$)

$$\hat{P}_g(u,x,s) = \sum_{n=0}^{\infty} c_n \phi_n^+(u) \exp[-(\alpha + \sqrt{n+s+\alpha^2})x] \tag{2.18}$$

obeying the boundary condition

$$\hat{P}_g(u,0,s) = g(u;s) \qquad \text{for } u > 0. \tag{2.19}$$

The expansion coefficients are given by

$$c_n = [\sqrt{8\pi}\, q_n]^{-1} \int_0^\infty du\, u \exp[-u^2/2] F_n^+(u) g(u). \tag{2.20}$$

The solution $\hat{P}_g$ is called the *albedo solution* of (2.2) for the boundary value g. Another important solution is the *Milne solution* $\hat{P}_M(u, x)$. For $\alpha \geqslant 0$ it describes the case where a constant current flows towards the absorbing wall from infinity; it can be written as

$$\hat{P}_M(u, x) = c' \phi_0^-(u) + \sum_{n=0}^{\infty} c_n \psi_n^+(u, x) \tag{2.21a}$$

with the boundary condition (for an absorbing wall)

$$\hat{P}_M(u, 0) = 0 \qquad \text{for } u > 0. \tag{2.21b}$$

The constant c' in (2.21a) is chosen such that the total current is unity. For the case $\alpha = s = 0$, $c'\phi_0^-(u)$ should be replaced by the function $\psi_0^c(u, x)$ defined in (2.12). One readily sees the connection between the two solutions: $\hat{P}_M - c'\phi_0^-$ is the albedo solution for $g(u) = -c'\phi_0^-(u)$, (for $\alpha = s = 0$, $\hat{P}_M - \psi_0^c$ is the albedo solution with $g(u) = \phi_0'(u)$ up to a constant).

It had been known for some time that the Milne and albedo solutions are non-analytic at $u = x = 0$ [10, 11]. Since the ϕ_n^+ are analytic functions, this implies that the sequences (2.18) and (2.21a) converge non-uniformly; the nature of the singularity follows from the asymptotic behaviour of the expansion coefficients c_n for large n. An alternative way of studying the behaviour of $\hat{P}$ near the singular point is by a transformation of variables; following [1] we introduce

$$\eta = -ux^{-1/3} \qquad \xi = x^{1/3} \tag{2.22}$$

and write the function $\hat{P}(u, x, s) = \hat{P}(\xi, \eta)$ (we suppress the dependence of s) as

$$\hat{P}(\xi, \eta) = \sum_\lambda \xi^\lambda f_\lambda(\eta) \tag{2.23}$$

with the λ still to be determined. The relations (2.22) imply the correspondences (for fixed ξ)

$$\eta = 0 \Leftrightarrow u = 0, x > 0 \qquad \eta \to \pm\infty \Leftrightarrow (x \downarrow 0; \pm u < 0). \tag{2.24}$$

The requirement that $\hat{P}$ remain finite for $x \downarrow 0$ implies the growth condition (for $\lambda \geqslant 0$)

$$f_\lambda(\eta) = \mathcal{O}(|\eta|^\lambda) \qquad \text{for } |\eta| \to \infty. \tag{2.25}$$

In the new variables, (2.2) and (2.3), combined with (2.23), lead to the recursion relations

$$-\eta f_{\lambda-2}' + 2\alpha f_{\lambda-1}' - (1-s) f_{\lambda-2} = \mathcal{L}_\lambda f_\lambda \tag{2.26}$$

with

$$\mathcal{L}_\lambda f_\lambda = \left(\frac{\partial^2}{\partial \eta^2} - \frac{\eta^2}{3} \frac{\partial}{\partial \eta} + \frac{\eta\lambda}{3} \right) f_\lambda. \tag{2.27}$$

The lowest term in the expansion (2.23) should have as f_λ an eigenfunction of $\mathcal{L}_\lambda$ with eigenvalue zero, denoted by $\chi_\lambda(\eta)$. Using the relation between $\mathcal{L}_\lambda$ and the differential operator appearing in the confluent hypergeometric equation [20], realized by the

transformation $z=\eta^3/9$, one sees that a solution obeying the constraint (2.25) is

$$\chi_\lambda(\eta)=3^{2\lambda/3}U\left(\frac{-\lambda}{3},\frac{2}{3},\frac{\eta^3}{9}\right)$$

$$U(a,c\,z)=\frac{\Gamma(1-c)}{\Gamma(a+c+1)}{}_1F_1(a,c,z)+z^{1-c}{}_1F_1(a-c+1,2-c,z)\frac{\Gamma(c-1)}{\Gamma(a)} \tag{2.28}$$

with ${}_1F_1(a,c,z)$ the confluent hypergeometric function, and the prefactor in χ_λ chosen for convenience. Asymptotically for large $|\eta|$ one has

$$\chi_\lambda(\eta)\sim\eta^\lambda{}_2F_0\left(\frac{-\lambda}{3},\frac{1-\lambda}{3},\frac{-9}{\eta^3}\right)=\eta^\lambda\left[1+\frac{\lambda(1-\lambda)}{\eta^3}+\mathcal{O}(\eta^{-6})\right]\qquad\text{for }\eta\to+\infty \tag{2.29a}$$

$$\chi_\lambda(\eta)\sim(-\eta)^\lambda 2\sin\left(\frac{\pi}{6}-\frac{\lambda\pi}{3}\right){}_2F_0\left(\frac{-\lambda}{3},\frac{1-\lambda}{3},\frac{-9}{\eta^3}\right)\qquad\text{for }\eta\to-\infty \tag{2.29b}$$

with ${}_2F_0$ a generalized hypergeometric function [20]. Once $\chi_\lambda(\eta)$ is known, the solution (2.23) with $\xi^\lambda\chi_\lambda$ as its first term can be constructed from (2.26) using the recursion relations for the confluent hypergeometric functions.

In the albedo problem, the function $\hat{P}(u,0,s)$ equals $g(u)$ for $u>0$, and hence the asymptotic behaviour of $\hat{P}(\xi,\eta)$ for $\eta\to-\infty$ is given: to each term in the Taylor series of $g(u)$ corresponds a definite solution of the type just discussed. However, in view of (2.29*b*), a solution starting with $\xi^{3m+1/2}\chi_{3m+1/2}(\eta)$ vanishes asymptotically for $\eta\to-\infty$ (as can be shown by working through the recursion scheme (2.27)). A linear combination of such solutions, discussed in more detail in the next section, can always be added without modifying the $\eta\to-\infty$ asymptotics; the coefficients in this linear combination have to be determined from other features of the solution, such as the values of the coefficients c_n in the expansions (2.18) or (2.21*a*). This procedure will be carried out in the three subsequent sections for various stationary Milne and albedo problems; a simple non-stationary problem will be discussed elsewhere [21]. For stationary problems, the Laplace variable s should be taken equal to zero; hence we shall suppress the variable s from now on, and omit the carets on $\hat{P}$ in the remainder of the paper.

3. The Milne problem with absorbing wall

The expansion (2.21) for the Milne problem is simplified greatly by the fact that the function $\phi_0^-(u)$ is itself one of the orthonormal set of functions (2.7) (recall that the Milne problem reduces to the albedo problem for ϕ_0^-). If one extends the integral (2.20) over the entire u-axis (which is allowed, since F_n^+ vanishes for $u<0$), and substitutes (2.15), only the term with σ_{n0} survives, and one obtains, for $s=0$, $\alpha>0$,

$$\hat{P}_M(u,x)=\frac{e^{-\alpha^2}}{\alpha\sqrt{8\pi}}\left\{\phi_0^-(u)-\sum_{n=0}^{\infty}\frac{\phi_n^+(u)\exp[-(\alpha+q_n)x]}{2(q_n+\alpha)q_nQ_nQ_0}\right\} \tag{3.1}$$

where we used the expression (2.16) for σ_{n0}. The prefactor follows from the normalization condition

$$c'\int_{-\infty}^{+\infty}du\,u\phi_0^-(u)=c'\int du\,u\exp[-\tfrac{1}{2}u^2-2\alpha u-\alpha^2]=-1. \tag{3.2}$$

The corresponding density profile $n_M(x)$ can be calculated using the expression

$$\int \mathrm{d}u\, \phi_n^{\sigma}(u) = \sqrt{\frac{2\pi}{n!}}\,(q_n+\sigma\alpha)^n \exp\left[\frac{\alpha^2-q_n^2}{2}-\sigma\alpha q_n\right] \tag{3.3}$$

which can be derived from the explicit expressions (2.5) using the representation

$$D_n(z) = (-1)^n\, \mathrm{e}^{z^2/4}\frac{\mathrm{d}^n}{\mathrm{d}z^n}\mathrm{e}^{-z^2/2} \tag{3.4}$$

and repeated integrations by part.

For large x, only the $n=0$ term in the sum in (3.1) survives, and the density profile becomes

$$\tilde{n}_M(x) = \frac{1}{2\alpha}\left[1-\frac{\mathrm{e}^{-2\alpha^2-2\alpha x}}{4\alpha^2 Q_0^2(\alpha^2)}\right]. \tag{3.5}$$

If we define the *Milne length* $x_M(\alpha)$ by the relation

$$\left.\frac{\mathrm{d}\tilde{n}_M(x)}{\mathrm{d}x}\right|_{x=0} = \frac{1}{x_M(\alpha)}\,\tilde{n}_M(x=0) \tag{3.6}$$

we obtain for this coefficient in the effective boundary condition to be imposed on the asymptotic density profile $\tilde{n}_M(x)$

$$x_M(\alpha) = \frac{1}{2\alpha}\left[4\alpha^2 Q_0^2(\alpha^2)\,\mathrm{e}^{2\alpha^2}-1\right] \tag{3.7}$$

where the function $Q_0(\alpha^2)$ was defined in (2.17). For positive α the Taylor series of its logarithm is given by [1]

$$\ln Q_0(\alpha^2) = -\ln 2\alpha - \sum_{m=0}^{\infty}\cdot\frac{(-1)^m\Gamma(m+1/2)\zeta(m+1/2)}{m!\,\Gamma(1/2)(2m+1)}\,\alpha^{2m+1} \tag{3.8}$$

where $\zeta(z)$ denotes the Riemann ζ-function. For small α one has

$$Q_0(\alpha^2) \sim \frac{1}{2\alpha}\left[1-\alpha\zeta(1/2)+\mathcal{O}(\alpha^2)\right] \tag{3.9}$$

from which one finds [1] by substitution in (3.7)

$$x_M(0) = -\zeta(1/2) = 1.460\,354\,5088\ldots. \tag{3.10}$$

For the full density profile $n_M(x)$ one finds using (3.1) and (3.3)

$$n_M(x) = \frac{1}{2\alpha} - \sum_{n=0}^{\infty} a_n(\alpha)\exp[-(\alpha+q_n)x] \tag{3.11a}$$

$$a_n(\alpha) = \frac{(q_n+\alpha)^{n-1}\exp[-n/2-\alpha q_n-\alpha^2]}{4\alpha Q_n Q_0\sqrt{n!}}. \tag{3.11b}$$

As mentioned in the preceding section, the behaviour for small x depends on the asymptotic behaviour of the $a_n(\alpha)$ for large n, which can be determined using the asymptotic expression

$$a_n(\alpha) \sim \frac{(2\pi)^{-3/4}\,\mathrm{e}^{-\alpha^2}}{4\alpha Q_0}\,n^{-5/4} \times\left\{1+\left[\zeta\left(-\frac{1}{2},\alpha^2\right)-\alpha\left(\frac{2\alpha^2}{3}+1\right)\right]n^{-1/2}+\mathcal{O}(n^{-1})\right\} \tag{3.12}$$

which is obtained from (3.11*b*) by using Stirling's formula and the asymptotic expansion for large n [1]

$$\ln Q_n(\alpha^2) \sim \ln\sqrt{2\pi} - \sum_{k=0}^{\infty} \frac{\zeta(-k-1/2, \alpha^2)}{2k+1} q_n^{-2k-1}. \tag{3.13}$$

In (3.12) and (3.13) the function $\zeta(z, a)$ is the generalized ζ-function, defined as (the analytic continuation of)

$$\zeta(z, a) = \sum_{k=0}^{\infty} (k+a)^{-z}. \tag{3.14}$$

Substitution of (3.13) into (3.11*a*) and Taylor expansion of the q_n around $\sqrt{n}$ finally yields the non-analytic part of $n_M(x)$ for small x as a linear combination of expressions of the type

$$f(x; a) \equiv \sum_{n=1}^{\infty} n^{-a} e^{-x\sqrt{n}} \sim 2\Gamma(2-2a)x^{2a-2} + \sum_{n=0}^{\infty} \zeta(a-n/2)\frac{(-x)^n}{n!}. \tag{3.15}$$

In general, the second contribution is analytic, hence unimportant for the singularity structure. However, for $a = 1+k/2$, the first term and a term in the sum both diverge ($\zeta(x)$ has a pole at $x=+1$); they compensate, but leave a logarithmic residue [see section 4]. For small x we obtain for the density profile $n_M(x)$

$$n_M(x; \alpha) = n_M(0; \alpha) + \frac{(2\pi)^{1/4} e^{-\alpha^2}}{2\alpha Q_0(\alpha^2)}\sqrt{x} + \mathcal{O}(x) \tag{3.16}$$

where $n_M(0; \alpha)$ contains non-asymptotic contributions.

In our discussion of the singular structure of the full solution we shall need the behaviour of $P_M(0, x)$ for small x; this is determined similarly to (3.16), using the asymptotic expression for the parabolic cylinder function $D_n(x)$ near its point of inflection [20]:

$$\phi_n^+(0) = \frac{1}{\sqrt{n!}} D_n(2q_n) \sim \frac{\Gamma(1/3)}{3^{1/6}(2\pi)^{3/4}} n^{-1/12} + \mathcal{O}(n^{-5/12}). \tag{3.17}$$

If we substitute this into the original expression (3.1), and note that q_n becomes of order $n^{1/2}$, whereas Q_n approaches a constant in view of (3.13), we see that the dominant non-analytic contribution to $P_M(0, x)$ involves the function $f(x; 13/12)$, and obtain

$$P_M(0, x) = \frac{(3)^{5/6}\Gamma(1/3)\exp[-\alpha^2]}{\alpha Q_0(\alpha^2)(2\pi)^{3/4}\Gamma(1/6)} x^{1/6} + \mathcal{O}(x^{5/6}). \tag{3.18}$$

The vanishing of the constant term is best shown by means of the inner expansion. For later reference we note that, in contrast to (3.16), the first correction is also non-analytic, hence derivable from the asymptotics.

Before turning to results obtained by means of the inner expansion, we mention the special form the above results take for the case of a vanishing external potential in (2.1), $\alpha = 0$, and report a few results obtained by numerical evaluation of our expressions. From (3.1) one finds for the full solution in the special case $\alpha = 0$, applying the expression (2.12) for the current-carrying solution and the expression (3.9) for $Q_0(\alpha^2)$ at small α,

$$P_M(u, x) = \frac{e^{-u^2/2}}{\sqrt{2\pi}}\left[x - u - \zeta\left(\frac{1}{2}\right) - \frac{1}{2}\sum_{n=1}^{\infty} \frac{f_n^+(u)}{nQ_n} e^{-x\sqrt{n}}\right]. \tag{3.19}$$

For the density profile at small x one similarly obtains

$$n_M(x) = n_M(0) + \left(\frac{2}{\pi}\right)^{1/4} \sqrt{x} + \mathcal{O}(x). \tag{3.20}$$

As in (3.16), $n_M(0)$ contains non-asymptotic information; a numerical evaluation of (3.18), in which the first Q_n are calculated explicitly and higher ones are replaced by an asymptotic value from (3.13), yields

$$n_M(0) = 0.936\,1145\ldots. \tag{3.21}$$

By similar numerical methods we determined the complete density profiles for various α. In figure 1 we give the deviation of the complete profile from the Chapman-Enskog part (3.5), normalized by the latter, i.e. the density depletion in the boundary layer. We see that this function decreases only slightly for not too small α (note that $\alpha = 0.1$ corresponds to a drift velocity in the stationary state equal to 20% of the thermal velocity, as is clear from (2.5) and (2.6)). For high α, where the drift velocity is very large, the boundary layer becomes much less pronounced.

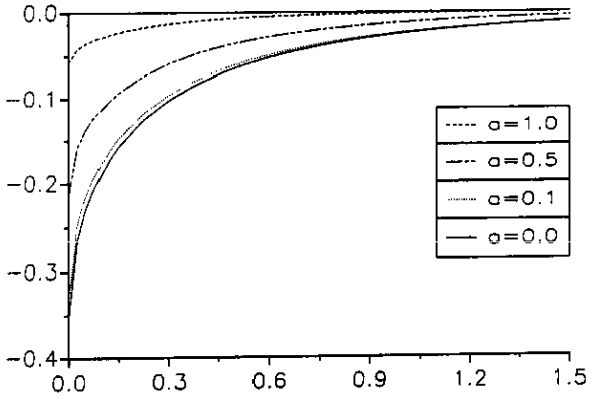

Figure 1. The boundary layer part of the density profile, $n_M(x) - \tilde{n}_M(x)$, with $\tilde{n}_M(x)$ the asymptotic part of the solution given by (3.5), divided by $\tilde{n}_M(x)$, for the Milne problem in a constant external field. The curves correspond to several values of the field parameter α, where 2α is the stationary drift velocity in units of the thermal velocity $(m\beta)^{-1/2}$. The length scale is the velocity persistence length $l = \gamma^{-1}(m\beta)^{-1/2}$, with γ the friction coefficient.

To determine the velocity distribution $P_M(u, 0)$ at the wall for small u we use the inner expansion method, described at the end of section 2. We shall employ special solutions of type (2.23), in which the function $f_\lambda(\eta)$ multiplying the lowest power of ξ equals the χ_λ introduced in (2.25); higher terms in the expansion (2.23) are determined from the recursion (2.26) in such a way that no eigenfunctions of $\mathcal{L}_{\lambda+k}$ with eigenvalue zero are added in order $\xi^{\lambda+k}$. The solution so constructed is denoted by $\Xi_\lambda(\xi, \eta)$. It then follows from the boundary condition (2.21*b*) (the vanishing of $P_M(u, 0)$ for $u > 0$) and from the asymptotics (2.29*b*) that only Ξ_λ with $\lambda = 3m + 1/2$ can occur. We may therefore write

$$P_M(\xi, \eta) = \sum_{k=0}^{\infty} d_k(\alpha) \Xi_{3k+1/2}(\xi, \eta). \tag{3.22}$$

The function $P_M(u, 0)$ is obtained by letting η go to infinity in such a way that $\xi\eta = -u$ stays constant. For general α the result is

$$P_M(-u, 0) = d_0(\alpha)\sqrt{u}\,[1 + \alpha u + \tfrac{9}{20}(2\alpha^2 - 1)u^2] + \mathcal{O}(u^{7/2}). \tag{3.23}$$

The coefficient $d_0(\alpha)$ is determined by calculating $P_M(0, x) = P_M(0, \xi^3)$. For this quantity we obtain from (3.22) and the definition of Ξ_λ

$$P_M(0, x) = d_0(\alpha)\chi_{1/2}(0)x^{1/6} + \mathcal{O}(x^{5/6}) \tag{3.24}$$

and a comparison with (3.18) gives

$$d_0(\alpha) = \frac{\sqrt{3}\exp[-\alpha^2]}{(2\pi)^{3/4}\alpha Q_0(\alpha^2)}. \tag{3.25}$$

For the special case $\alpha = 0$ we carried the calculations somewhat further and obtained

$$P_M(-u, 0) = d_0 u^{1/2}(1 - \tfrac{9}{20}u^2 + \tfrac{123}{1120}u^4) + d_1 u^{7/2}(1 - \tfrac{15}{44}u^2) + \mathcal{O}(u^{13/2}) \qquad (\alpha = 0). \tag{3.26}$$

For $P_M(0, x)$ we obtain

$$P_M(0, x) = d_0[\chi_{1/2}(0)x^{1/6} + 3/5\chi'_{1/2}(0)x^{5/6}] + d_1\chi_{7/2}(0)\chi^{7/6} + \mathcal{O}(x^{11/6}) \qquad (\alpha = 0) \tag{3.27}$$

and a comparison with (3.18), also carried two orders further, yields

$$d_0 = 2\sqrt{3}\,(2\pi)^{-3/4} = 0.872\,882\ldots \tag{3.28a}$$

$$d_1 = \tfrac{8}{35}\sqrt{3}\,(2\pi)^{-3/4}\zeta(-\tfrac{1}{2}) = -0.020\,738\ldots. \tag{3.28b}$$

The distributon function (3.26) is shown in figure 2, together with results from a numerical simulation [17] and from two versions of the moment method [8, 13]. The small-u asymptotic result (3.26) agrees well with the simulation till close to $|u| = 1$ (the deviations at small u are systematic errors in the simulation [17]). For large $|u|$ both moment methods agree well with the simulation; they also show good convergence with the number of moments in that region (see e.g. figure 1 of [8]). The two-stream moment method [13], a generalization of a procedure first applied to the present problem by Razi Naqvi *et al* [22], shows remarkably good results down to very low $|u|$, where the singularity is replaced by a finite jump.

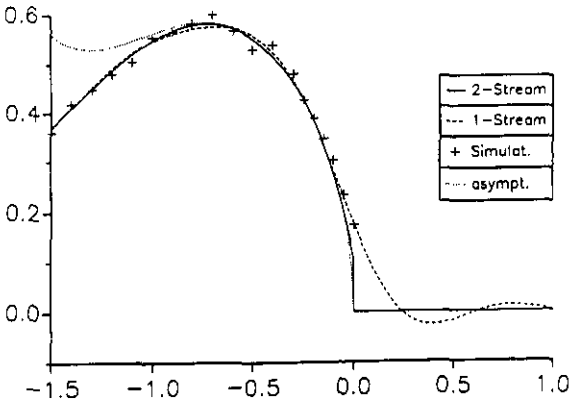

Figure 2. The velocity distribution $P(u, 0)$ at the wall for the Milne problem without external force, as calculated by the exact asymptotic expansion near $u = 0$, by two variants of the moment method [8, 13], and by numerical simulation [17].

4. Stationary albedo problems

In this section we shall consider various stationary albedo problems for the field free case, i.e. we consider the problem (2.18) with $s=\alpha=0$. If we assume the function $g(u)=P(u,0)$ for $u>0$ to have an expansion of the form

$$g(u)=u^a\sum_{k=0}^{\infty}g_k u^k \tag{4.1}$$

then the albedo solution $P_g(u,x)$ in the variables ξ and η must have the form

$$P_g(\xi,\eta)=\sum_{k=0}^{\infty}g_k\frac{\Xi_{a+k}(\xi,\eta)}{2\sigma_{a+k}}+\sum_{j=0}^{\infty}d_j(g)\Xi_{3j+1/2}(\xi,\eta) \tag{4.2}$$

with the functions Ξ_λ defined in the text preceding (3.22) and

$$\sigma_a=\sin\left[\frac{\pi}{6}(1-2a)\right]. \tag{4.3}$$

The first contributions in (4.2) ensure the right asymptotics for $\eta\to\mp\infty$ (determined by the behaviour of $P(u,0)$ for $u>0$)); the second sequence of contributions vanishes for $x=0$, $u>0$; therefore the $d_j(g)$ cannot be calculated from the inner expansion. As in the Milne solution, they must be determined by an asymptotic analysis of the expansion coefficients c_n in the expansion (2.18) of P_g in terms of the $f_n^+(u)$. Before discussing the determination of the $d_n(g)$, we first discuss the solution $P_g(u,0)$ for small negative u. From the explicit expressions (2.29) and the results in the preceding section one has (for $a\neq k+\frac{1}{2}$)

$$\begin{aligned}P_g(-u,0)=&\frac{g_0u^a}{2\sigma_a}+\frac{g_1u^{a+1}}{2\sigma_{a+1}}+\left[\frac{g_2}{2\sigma_{a+2}}-\frac{g_0(a+4)}{8(a+2)}\left(\frac{1}{\sigma_a}-\frac{1}{\sigma_{a+2}}\right)\right]u^{a+2}\\&+d_0(g)u^{1/2}(1-\tfrac{9}{20}u^2)+d_1(g)u^{7/2}+\mathcal{O}(u^{9/2},u^{a+3})\end{aligned} \tag{4.4}$$

with σ_k defined in (4.3). Note that for $a<\frac{1}{2}$ the dominant singularity for negative u is of type $u^{1/2}$. For $a>\frac{1}{2}$ it is of type $u^{1/2}$. For $a\to k+\frac{1}{2}$ one of the σ_a vanishes; as we shall see, this will be compensated by a similar divergence in the $d_i(g)$ in front of the same power of u.

The determination of the asymptotic behaviour of the c_n, which must be calculated to determine the $d_i(g)$, is considerably more complicated than in the Milne case. For definiteness, we shall discuss the special case

$$g(u)=u^a\exp[-bu^2/2]. \tag{4.5}$$

This general form includes, for $a=0$, the important case of thermal emission with a temperature not necessarily equal to the background temperature. Moreover, the class of functions (4.5) includes representatives of all the types of singular behaviour encountered in (4.4), but is sufficiently simple to allow at least some of the steps in the calculations to be performed analytically. With $g(u)$ given by (4.5), the c_n for $n>0$ are given by (see (2.20) and (2.15))

$$c_n=\frac{1}{\sqrt{8\pi n}}\left[I_{n+}-\frac{\Gamma(1+a/2)}{2\sqrt{n}\,Q_n(b/2)^{1+a/2}}-\frac{1}{2Q_n}\sum_{m=1}^{\infty}\frac{I_{m-}}{Q_m\sqrt{m}\,(\sqrt{m}+\sqrt{n})}\right] \tag{4.6}$$

with

$$I_{n\sigma}=\frac{2^{-n/2}\,\mathrm{e}^{-n}}{\sqrt{n!}}\int_0^\infty \mathrm{d}u\,u^{a+1}\,\mathrm{e}^{-bu^2/2+\sigma u\sqrt{n}}H_n(\sqrt{2n}-\sigma u/\sqrt{2}). \tag{4.7}$$

The second term in (4.6) represents the $m=0$ term in (2.15), with the $\alpha \downarrow 0$ limit taken using (3.9) and (2.5). The $I_{n\sigma}$ can be evaluated asymptotically for large n using the techniques explained in [10]. The result is

$$I_{m-} \sim (2\pi)^{1/4} M|\mathrm{Ai},\, a+2|\, m^{-5/12-a/6}[1+\mathcal{O}(m^{-1/3})] \tag{4.8a}$$

$$I_{m+} \sim 2\vartheta_a (2\pi)^{1/4} M|\mathrm{Ai},\, a+2|\, m^{-5/12-a/6}[1+\mathcal{O}(m^{-1/3})] \tag{4.8b}$$

where $M|\mathrm{Ai}, x|$ denotes the Mellin transform of the Airy function

$$M|\mathrm{Ai}, z| = \int_0^\infty \mathrm{d}t\, t^{z-1}\, \mathrm{Ai}(t) = \frac{1}{2\pi} 3^{(4z-7)/6} \Gamma\left(\frac{z}{3}\right) \Gamma\left(\frac{z+1}{3}\right). \tag{4.9}$$

Asymptotic evaluation of c_n therefore requires asymptotic evaluation of expressions of the type

$$R_n(x) = \sum_{m=1}^{\infty} m^{-x}[\sqrt{m}+\sqrt{n}]^{-1}. \tag{4.10}$$

This expression can be evaluated using the techniques explained in appendix 3 of [1]. For non-integer values of $2x$ the result is

$$R_n(x) \sim \frac{-2\pi n^{1/2-x}}{\sin(2\pi x)} + \sum_{j=0}^{\infty} (-1)^j n^{-(j+1)/2} \zeta(x-j/2). \tag{4.11}$$

For the special case $a=\frac{1}{2}$, one needs $R_n(\frac{3}{2})$. At $x=\frac{3}{2}$ the first term and the $j=1$ term in the sum become singular; the singularity is removable and the result is

$$R_n(\tfrac{3}{2}) \sim -n^{-1}(c_{\mathrm{E}} + \ln n) + \sum_{j=0}^{\infty}{}' (-1)^j n^{-(j+1)/2} \zeta[(3-j)/2] \tag{4.12}$$

where c_{E} is Euler's constant and the prime indicates that the term $j=1$ should be omitted. Using the above results one finds for the c_n asymptotic expansions of the type

$$c_n = \Omega_0 n^{-1} + \Omega_1 n^{-3/2} + \Omega_2 n^{-11/12-a/6} + \Omega_3 n^{-15/12-a/6} + \mathcal{O}(n^{-2}, n^{-19/12-a/6})$$
$$\text{for } a \neq k+\tfrac{1}{2} \tag{4.13}$$

$$c_n = \omega_0 n^{-1} + \omega_1 n^{-3/2} + \omega_2 n^{-1} \ln n + \omega_3 n^{-4/3} + \mathcal{O}(n^{-5/3}) \qquad \text{for } a = \tfrac{1}{2}. \tag{4.14}$$

The coefficients Ω_0 and Ω_1, or ω_0 and ω_1, contain the non-asymptotic values of the I_{m-}, and must therefore be evaluated numerically. For Ω_2 and Ω_3 we obtain

$$\begin{aligned} \Omega_2 &= \frac{M|\mathrm{Ai},\, a+2|}{(2\pi)^{1/4}} [\vartheta_a - (4\vartheta_a)^{-1}] \\ \Omega_3 &= \frac{a+1}{2} [(\tfrac{1}{2}-b)(a+2)+1] \frac{M|\mathrm{Ai},\, a+1|}{(2\pi)^{1/4}} [\vartheta_{2+a} - (4\vartheta_{2-a})^{-1}]. \end{aligned} \tag{4.15}$$

In particular, Ω_2 vanishes for $a=3j$ or $a=3j+1$, as is clear from (4.3), and Ω_3 for $a=3j+1$ or $a=3j+2$; as we saw before, Ω_2 diverges for $a=\frac{1}{2}$.

An analysis as in the previous section relates Ω_0 and Ω_1 to the as yet unknown coefficients in P_g, given in (4.2):

$$d_0 = -4\sqrt{3}\,(2\pi)^{1/4} \Omega_0 \qquad d_1 = -\tfrac{16}{35}\sqrt{3}\,(2\pi)^{1/4} \Omega_1. \tag{4.16}$$

The values for d_0 as a function of a for several values of b are given in figure 3. For $a=0$, $b=1$ one finds $d_0=0$, as it should be, since in that case $P_g(u,x) = \phi_0(u)$, as one

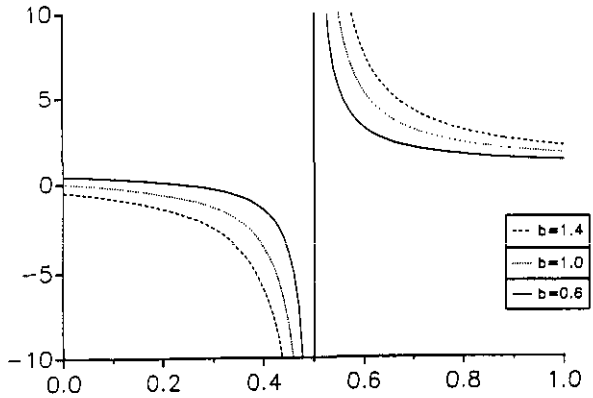

Figure 3. The coefficient $d_0(a, b)$ of the $u^{1/2}$ contribution to the velocity distribution at the wall at small negative velocities for the albedo problem with injected distribution $g(u) = u^a \exp[-bu^2/2]$, as a function of the parameter a for several values of b.

sees easily by substitution. The poles in d_a for $a = \frac{1}{2}$ are also clearly visible in the figure. For $a = \frac{1}{2}$, ω_2 and ω_3 can be calculated in closed form. From (4.14) we obtain instead of (4.4) the distribution

$$P_g(-u, 0) = \frac{-3}{2\pi}\sqrt{u}\ln u + \tilde{d}_0\sqrt{u} + \frac{27}{40\pi}u^{5/2}\ln u + \mathcal{O}(u^{5/2}) \tag{4.17}$$

where $\tilde{d}_0$ contains the non-singular contributions from the coefficients of $\sqrt{u}$ in (4.4) for $a = \frac{1}{2}$.

The density profile $n_g(x)$ can be calculated using the methods explained for the Milne solution in the preceding section. The general expression for small x is

$$n_g(x) = n_g(0) - 4(2\pi^3)^{1/4}\Omega_0\sqrt{x} - \frac{6\Gamma((2-a)/3)}{a+1}(2\pi)^{1/4}\Omega_2 x^{(1+a)/3} + \mathcal{O}(x)$$
$$\text{for } 0 < a < 2 \qquad 2a \text{ non-integer} \tag{4.18}$$

where $n_g(0)$ contains non-asymptotic contributions. For $a = 0$, Ω_2 vanishes, as is clear from (4.15); and we obtain

$$n_g(x) = n_g(0) - 4(2\pi^3)^{1/4}\Omega_0\sqrt{x} + 2(2\pi)^{1/4}\Omega_3 x\ln x + \mathcal{O}(x) \tag{4.19}$$

where the logarithmic term is caused by compensating singularities in (3.15). The quantity Ω_0 is negative for $b < 1$ (injected particles hotter than the background) and positive thereafter. Results for the full profiles $n_g(x)$ for $a = 0$ and several values of b (thermal injection at temperatures different from the background temperature) are given in figure 4. As was seen already in [8], the density at infinity increases with increasing temperature of the injected particles (the injection become more 'effective' with increasing average injection velocity). For the special value $a = \frac{1}{2}$ the density profile also obtains logarithmic contributions:

$$n_g(x) = n_g(0) - \frac{\sqrt{x}\ln x}{\sqrt{12\pi}} - 4(2\pi^3)^{1/4}\sqrt{x}\left[\omega_0 + \frac{c_E + 2(\ln 2 - 1)}{4\sqrt{3}\,(2\pi)^{5/4}}\right] + \mathcal{O}(x). \tag{4.20}$$

In conclusion, we have seen that the leading singularities in P_g at $u = x = 0$ depend on the exponent a. For $0 < a < \frac{1}{2}$, $P_g(u, 0)$ at small u is of order $|u|^a$ for both positive and negative u, and the density profile has a term $x^{(1+a)/3}$ as the leading sigularity.

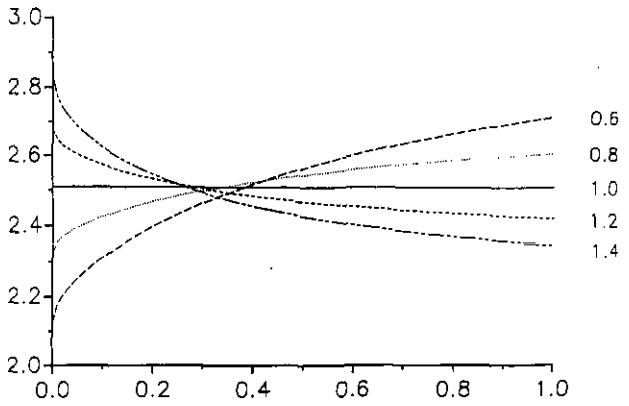

Figure 4. The density profile for the albedo problem with injected velocity distribution $g(u)=\exp[-bu^2/2]$ for several values of b. For $b=1$ (injection with a Maxwellian at the background temperature) the equilibrium distribution with density $\sqrt{2\pi}$ results.

For $a>\frac{1}{2}$, the leading singularity in $P_g(-|u|,0)$ is of type $\sqrt{|u|}$, and that in $n_g(x)$ is of type $\sqrt{x}$. At the crossover point $a=\frac{1}{2}$, logarithmic corrections to both singularities appear. For $a\downarrow 0$ the leading singularity disappears; $P_g(u,0)$ remains continuous at $u=0$, and the density profile retains only a weak singularity of type $x\ln x$.

5. The Milne problem for partially reflecting walls

When the wall reflects some of the particles impinging upon it, the boundary condition at $x=0$ takes the form

$$uP(u,0)=\int_{u'<0} \mathrm{d}u'|u'|\mathscr{R}(u\,|\,u')P(u',0) \qquad \text{for } u>0 \tag{5.1}$$

where $\mathscr{R}(u\,|\,u')$ denotes the probability that a particle arriving at the wall with velocity u' is reflected with velocity u. For a partially reflecting wall, the integral of $\mathscr{R}$ over u is less then unity. The Marshall–Watson procedure for Milne problems with boundary conditions of this types becomes very complicated; it involves inverting a matrix formed by matrix elements of $\mathscr{R}$ between the $f_n^\sigma(u)$. Therefore, it will in practice always be preferable to solve such problems by moment methods, and use the methods discussed in this paper only for analysis of the singularity. As an example we shall consider in this section the case of partial specular reflection with a velocity-independent reflection coefficient:

$$P_r(u,0)=rP_r(-u,0) \qquad \text{for } u>0. \tag{5.2}$$

If we construct the inner expansion (2.23) for P_r, the starting powers λ should obey the relation, seen from the asymptotic behaviour (2.29),

$$r=2\sigma_\lambda=2\sin(\pi/6-\lambda\pi/3) \tag{5.3}$$

with the solutions

$$\begin{aligned}\lambda_k&=6k+\frac{1}{2}-\frac{3}{\pi}\sin^{-1}(r/2)\\ \mu_k&=6k+\frac{7}{2}+\frac{3}{\pi}\sin^{-1}(r/2).\end{aligned} \tag{5.4}$$

If we denote λ_0 and μ_0 by λ and μ, the result obtained by solving the first few terms of the recursions (2.26) can be written as

$$P_r(-u,0) = d_0(r)u^{\lambda}\left\{1-\frac{\lambda+4}{4(\lambda+2)}u^2+\frac{u^4}{4(\lambda+2)}\left(1+\frac{(\lambda+2)(5\lambda+3)}{40(\lambda+3)}\right)\right\}$$
$$+d_1(r)u^{\mu}\left\{1-\frac{\mu+4}{4(\mu+2)}u^2\right\}+\mathcal{O}(u^{\lambda+6}) \qquad \text{for } u>0. \tag{5.5}$$

The result for positive u follows from (5.2). For $r\downarrow 0$ the functions $d_0(r)$ and $d_1(r)$ should approach the values d_0 and d_1 for the pure Milne problem, given in (3.28). For $r\to 1$ the distribution $P_r(-u,0)$ should approach to a multiple of the Maxwell distribution. From the normalization to unit current one finds

$$\lim_{r\to 1}(1-r)P_r(-u,r)=\phi_0(u)=\exp[-u^2/2] \qquad \text{for } u>0. \tag{5.6}$$

In this limit, λ and μ approach 0 and 4, respectively, and a comparison with (5.5) yields

$$\lim_{r\to 1} d_0(r)(1-r)=1 \qquad \lim_{r\to 1} d_1(r)(1-r)=-\tfrac{1}{160}. \tag{5.7}$$

From (3.28) and (5.7) we see that d_1 is much smaller than d_0 both for $r\downarrow 0$ and $r\to 1$; in addition, the term with $d_1(r)$ in (5.5) only becomes relevant for values of $|u|$ for which the asymptotic expansion becomes irrelevant anyhow. We therefore compared the results of the two-stream moment method [13] with the d_0-term in (5.5), using $d_0(r)$ as an adjustable parameter. The results for $r=0.25$ and $r=0.8$ are shown in figure 5. Clearly, there is a considerable range of u-values for which the agreement is very good. Near $u=0$, the finite jump imposed by the two-stream method can provide only a rough approximation to the actual singularity; in particular the zero at $u=0$ is not reproduced. The values for $d_0(r)$ that give the best fit agree to within numerical accuracy (three significant figures) with the expression

$$d_0(r)\approx d_0(0)+r/(1-r). \tag{5.8}$$

The numerical accuracy of the two-stream method did not suffice to provide an estimate for $d_1(r)$.

Before discussing a way of determining the $d_i(r)$, at least in principle, we mention that the asymptotic behaviour of the expansion coefficients $c_n(r)$ in the analogue of (2.21) is given by

$$c_n(r)\sim a_0(r)n^{-11/12-\lambda(r)/6}+a_1(r)n^{-11/12-\mu(r)/6}+\ldots \tag{5.9a}$$

with

$$a_0(r)=-\frac{(1-r^2)}{2(2\pi)^{1/4}}M|\mathrm{Ai},\lambda(r)+2|\,d_0(r) \tag{5.9b}$$

$$a_1(r)=-\frac{(1-r^2)}{2(2\pi)^{1/3}}M|\mathrm{Ai},\mu(r)+2|\,d_1(r). \tag{5.9c}$$

The corresponding asymptotic behaviour for the density profile is

$$n_r(x)=n_r(0)+\frac{3\Gamma((2-\lambda)/3)(1-r^2)M|\mathrm{Ai},\lambda+2|}{(1+\lambda)}x^{(1+\lambda)/3}d_0(r)+\mathcal{O}(x). \tag{5.10}$$

Thus, the exponent decreases from $\frac{1}{2}$ to $\frac{1}{3}$ as r varies from 0 to 1, with the coefficient going to zero in the latter limit. Note, however, that the term $n_r(0)$ approaches $\sqrt{2\pi}/(1-r)$ for $r\to 1$, whereas the second term (and the further corrections) remain finite in that limit.

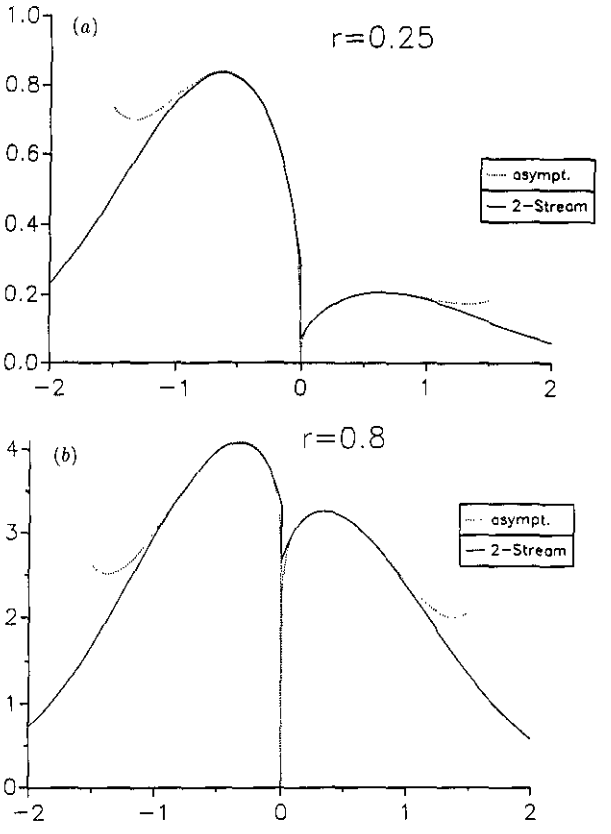

Figure 5. (*a*) The velocity distribution at the wall for the force-free Milne problem with partial specular reflection, as calculated from the exact asymptotic expansion near $u = 0$ and from the two-stream moment method, for the value $r = 0.25$ of the reflection coefficient. (*b*) The same quantities for reflection coefficient $r = 0.8$.

At least in principle, the $d_i(r)$ can be calculated by writing $P_r(u, x)$ as a power series in the reflection coefficient r[23]:

$$P_r(u, x) = \sum_{k=0}^{\infty} r^k P^{(k)}(u, x). \tag{5.11}$$

The separate terms represent particles that have been reflected precisely k times by the wall. They can therefore be interpreted as Milne ($k = 0$) and albedo solutions:

$$P^{(0)} = P_M \qquad P^{(i)} = P_g \text{ with } g(u) = P^{(i-1)}(-u, 0). \tag{5.12}$$

The same decomposition should also hold for the leading singularities in $P_r(-u, 0)$

$$d_0(r)u^{\lambda(r)} = \sum_{k=0}^{\infty} r^k f^{(k)}(u) \tag{5.13}$$

where the $f^{(k)}$ are obtained by combining the Taylor series

$$d_0(r) = d_0(0) + \sum_{k=1}^{\infty} r^k d_{0,k} \tag{5.14}$$

where the conjecture (5.8) would correspond to

$$d_{0,k} = 1 \qquad \text{for } k \geqslant 1 \tag{5.15}$$

and

$$u^{\lambda(r)} = \sqrt{u}\exp\left[-\left\{\frac{3}{\pi}\sin^{-1}\left(\frac{r}{2}\right)\right\}\ln u\right]$$

$$= \sqrt{u}\sum_{n=0}^{\infty} r^n \sum_{m=0}^{n} [\ln u]^m c_m^{(n)} \tag{5.16}$$

with

$$c_m^{(n)} = \frac{(-1)^m}{m!\,n!}\left(\frac{3}{\pi}\right)^m \frac{\partial^m}{\partial r^n}\left[\sin^{-1}\left(\frac{r}{2}\right)\right]^m\Bigg|_{r=0}. \tag{5.17}$$

(Note that only terms with even $n-m$ are non-zero.) Thus, we find for the asymptotic behaviour of $P^{(k)}(-u, 0)$ the expression

$$P^{(k)}(-u, 0) \sim \sqrt{u}\sum_{n=0}^{k} d_{0,k-n} \sum_{m=0}^{n} c_m^{(n)}[\ln u]^m. \tag{5.18}$$

Since $P^{(k)}$ is the solution of an albedo problem with $P^{(k-1)}(-u, 0)$ as the input function, the successive $P^{(k)}$ can be calculated using the methods expounded in section 4. To calculate the asymptotic behaviour, we need to study albedo problems of the type

$$g(u) = \sqrt{u}\,[\ln u]^m[1 + \mathcal{O}(u^2)]. \tag{5.19}$$

A comparison with the derivations in section 4 shows that the only new element is that the Mellin transforms (4.9) should be replaced by expressions of the type

$$I[z; m] = \int_0^{\infty} \mathrm{d}t\, t^{z-1}[\ln t]^m \mathrm{Ai}(t) \tag{5.20}$$

which can be obtained from I_{z-} in (4.8) by taking the mth derivative with respect to z. In this way, all terms in (5.18) with the exception of the $m = n = 0$ term involving the new coefficient $d_{0,k}$ can be determined exactly, and we find agreement with (5.18) (see [14] for full details). The coefficients $d_{0,k}$ for $k > 0$, like the coefficient $\tilde{d}_0$ in (4.17), contain non-asymptotic information as well, and depend on the global behaviour of $P^{(k-1)}(-u, 0)$. To calculate it, one must evaluate slowly converging asymptotic series; determining $d_{0,i}$ to an accuracy better than a few per cent by this method requires excessive computational effort. For $d_{0,1}$ we find the value 0.98 with an estimated accuracy of a few per cent, compatible with the estimate (5.8) inspired by the moment method. Since the logarithmic corrections do not influence the global behaviour very much, it appears reasonable that all $d_{0,k}$ with $k > 0$ should have roughly the same value. Analogous results were found for the corresponding coefficient $\tilde{d}_0(b)$ for the albedo problem for the function

$$g(u) = \sqrt{u}\exp[-bu^2/2].$$

It remains close to unity for b up to about 1.4, but decreases somewhat for higher b. From (3.26) we see that the effective value of b for the calculation of $d_{0,1}$ has the value $\frac{9}{10}$; hence a value near unity for $d_{0,1}$ is not surprising. Moreover, the limiting law (5.7) implies that the $d_{0,k}$ should approach unity for $k \to \infty$. However, the nature of the calculation and the behaviour of the corresponding quantity $\tilde{d}_0(b)$ for large b make it somewhat unlikely that the estimate (5.8) should be exactly true.

6. Concluding remarks

In this paper we have explored the exact solution found by Marshall and Watson for boundary layer problems of the Klein–Kramers equation. We found a surprisingly rich variety of singularity structures in the various special problems treated in sections 3–5, and we saw that the techniques developed in [1–3] provide powerful means to determine these structures. Since these techniques involve extensive use of asymptotic expansions it is comforting to have some consistency checks available, such as the agreement between the two different approaches to the Milne problem with partial specular reflection, set forth in section 5. The reliance on asymptotic expansions, as well as the slow convergence of several other series encountered in our analysis, make it very difficult, however, to obtain very accurate numerical results for non-asymptotic quantities, except in some favourable cases, such as the classical Milne problem, where the Milne length in the absence of an external field is given exactly in closed form. Other non-asymptotic quantities, in particular density profiles and other moments of the distribution functions, are in general obtained more efficiently by approximate methods, i.e. by methods that do not give the solution in closed form, but as the limit of a sequence of approximations. Such sequences often converge more rapidly than the series encountered in the present paper, and they are easier to program for numerical computation. Examples are the moment methods described in [8, 13, 22], or variants of these methods to be found in earlier work quoted in these papers. Some other approximate methods are described in a recent paper by Coron [9]; related work was reviewed recently by Sone [24]. However, since neither the mathematical justification for the use of the moment methods, nor the assignment of confidence limits to the results obtained by them is entirely straightforward, the methods developed in [1–3], and further worked out in the present paper, provide a welcome check on these more 'practical' methods as well.

Though we have focused our attention in this paper on the technical mathematical problems involved in solving the Klein–Kramers equation, we wish to point out that this equation has important applications, for example in analysing the growth of liquid droplets from a gas mixture, in particular when the vapour molecules are much heavier than the molecules of the carrier gas [25–27]. Other applications occur in the theory of diffusion-controlled chemical reactions [28]. Most applications contain additional complications and involve the Klein–Kramers equation in spherical, rather than planar geometry, but the exact techniques discussed here were used, for example, to obtain a systematic expansion of the spherical boundary layer problem in terms of the inverse radius of the sphere around which the kinetic boundary layer is formed [29]. Moreover, most calculational techniques applied in these more complicated problems are best tested first for the planar case, for which by now such a wealth of exact and additional reliable information has become available.

Acknowledgments

This work was supported by the Austrian 'Fonds zur Förderung der Wissenschaftlichen Forschung'. It is a pleasure to thank Dr Dietmar Petrascheck for valuable advice on numerical procedures.

Note added in proof. A rigorous proof of the existence and uniqueness of the solution (2.18) for general α has been given in a recent preprint by C Cercignani and C Sgarra.

References

[1] Marshall T W and Watson E J 1985 *J. Phys. A: Math. Gen.* **18** 3531
[2] Duck P W, Marshall T W and Watson E J 1986 *J. Phys. A: Math. Gen.* **19** 3545
[3] Marshall T W and Watson E J 1987 *J. Phys. A: Math. Gen.* **20** 1345
[4] Klein O 1922 *Ark. Mat. Astron. Fys.* **16**(5) 1
[5] Kramers H A 1940 *Physica* 7 284
[6] Cercignani C 1988 *The Boltzmann Equation and its Applications* (Berlin: Springer)
[7] Duderstadt J J and Martin W R 1979 *Transport Theory* (New York: Wiley)
[8] Widder M E and Titulaer U M 1989 *J. Stat. Phys.* **56** 471
[9] Coron F 1990 *Transport Theory and Statistical Physics* **19** 89
[10] Titulaer U M 1984 *J. Stat. Phys.* **37** 589
[11] Titulaer U M 1985 *Phys. Lett.* **108A** 19
[12] Mayya Y S 1985 *J. Chem. Phys.* **82** 2033
[13] Kainz A J and Titulaer U M 1991 *J. Phys. A: Math. Gen.* submitted
[14] Kainz A J 1989 *Diploma Thesis* (Linz University) unpublished
[15] Pagani C D 1970 *Boll. Un. Mat. Ital.* **3**(4) 961
[16] Burschka M A and Titulaer U M 1981 J. Stat. Phys. **25** 569
[17] Selinger J V and Titulaer U M 1984 *J. Stat. Phys.* **36** 293
[18] Burschka M A and Titulaer U M 1982 *Physica* **112A** 315
[19] Beals R and Protopopescu V 1983 *J. Stat. Phys.* **32** 565
[20] Olver F W J 1974 *Asymptotics and Special Functions* (New York: Academic)
[21] Kainz A J and Titulaer U M in preparation
[22] Razi Naqvi K, Mork K J and Waldenstrøm S 1989 *Phys. Rev.* A **40** 3405
[23] Titulaer U M 1986 *Coherence, Cooperation and Fluctuations* ed F Haake, L M Narducci and D Walls (Cambridge: Cambridge University Press) p 35
[24] Sone Y 1991 *Rarefied Gas Dynamics Proc. 17th Int. Symp. on Rarefied Gas Dynamics (Aachen, 1990)* ed A E Beylich (Weinheim: VCH) p 489
[25] Widder M E and Titulaer U M 1990 *Physica* **167A** 663
[26] Widder M E and Titulaer U M 1991 *Physica* **173A** 125
[27] Lindenfeld M J and Shizgal B. 1983 *Phys. Rev.* A **27** 1657
[28] Calef D F and Deutch J M 1983 *Ann. Rev. Phys. Chem.* **34** 493
[29] Widder M E and Titulaer U M 1989 *J. Stat. Phys.* **55** 1109